Robotic Path Following in 3D Using a Guiding Vector Field

Yao, Weijia; Kapitaniuk, Iurii; Cao, Ming

Published in:
Proceedings of the 2018 IEEE Conference on Decision and Control (CDC)

DOI:
10.1109/CDC.2018.8619780

2018 IEEE Conference on Decision and Control (CDC)
Miami Beach, FL, USA, Dec. 17-19, 2018

Robotic Path Following in 3D Using a Guiding Vector Field

Weijia Yao, Yuri A. Kapitanyuk, Ming Cao

Abstract— **Path following serves as one of the most basic functions for industrial or mobile robots used in different scenarios. In this paper, a general 3D guiding vector field (GVF) is analyzed rigorously that extends the existing results on 2D GVFs. The desired 3D path is described by the intersection of two zero-level surfaces in their implicit forms, which can be used to describe various desired paths. Although the same path can be represented by the intersection of different surfaces, convergence to the path is not always guaranteed. However, under some mild assumptions, the existence of solutions and the local and global convergence results are proved rigorously for both bounded and unbounded desired paths. Examples and counter-examples from simulations further validate the theoretical results.**

I. Introduction

The robotic path following problem, as its name suggests, is to design appropriate control laws so that the output of the robotic system can follow the desired path. This is particularly useful in many applications involving industrial or mobile robots [1]. There are a number of approaches to solving the path following problem [2], e.g. pure pursuit, line-of-sight (LOS), nonlinear guidance law (NLGL), linear quadratic regulator (LQR) and vector-field-based path following. Based on the detailed analysis and thorough comparison of these methods, [2] concludes that the vector-field algorithm solves the path-following problem with the lowest cross-track error and requires the least control efforts among several tested algorithms.

The use of vector-field methods for guidance has been studied extensively during the last decade [3]–[9]. With these methods, a vector field is designed so that its integral curves approach the desired path and thus guide a robot to the predefined path asymptotically. The corresponding algorithm is practically easy to implement and can be intuitively understood. Despite the simple implementation, the rigorous analysis remains complicated and challenging. This is demonstrated in [6], [8] only for the conventional trajectories in the two-dimensional (2D) space, such as the circular and straight-line paths. The recent work [10] proposes and analyzes rigorously a 2D guiding vector field (GVF) for a nonholonomic robot to follow a smooth desired path defined in the implicit form. With additional assumptions, such as assuming fixed height for flying drones, the results developed for the 2D case can be used for the inherently three-dimensional (3D) robotic systems, such as aerial and underwater robots, but it greatly restricts its potential applications.

The problem of 3D vector-field path following has been considered in works [3]–[5], [9]. The general approach on how to design the vector field for navigation in n-dimensional space was proposed in [5]; however, the authors consider only the case that the set of critical points is repulsive. The works [3], [4], [9] present similar approaches to designing the 3D vector field for the control of the spatial motion. Although in these works, there are various seemingly different representations of the desired path and the vector-field, in general, the desired path can be described as an intersection of two surfaces and the vector-field consists of two components. The first component is orthogonal to the desired path, and it vanishes once the robot reaches the path. The second component is tangential to the path and, usually, it is calculated as the cross product of the gradient vectors normal to the surfaces defining the path. In all of these works [3], [4], [9], it is assumed that the workspace is free of critical points at which the gradient vectors degenerate. Generally speaking, this can only be guaranteed locally near the desired path.

Motivated by the discussion above, the main goal of this paper is to provide a unified approach to the local and global rigorous analysis of the 3D vector field for both bounded and unbounded desired paths. The focus is on the less-investigated questions of the existence of solutions and the convergence of the integral lines generated by the 3D vector field.

The remainder of this paper is organized as follows. Section II presents the problem formulation, with the introduction of the 3D guiding vector field and assumptions. Section III analyzes the convergence of trajectories based on the guiding vector field. In Section IV, several illustrative examples along with simulation results are elaborated. Finally, Section V concludes the paper and indicates the future work.

II. Problem Formulation

Notations: We denote the distance between a point $p_0 \in \mathbb{R}^3$ and a set $\mathcal{S} \subset \mathbb{R}^3$ by $\operatorname{dist}(p_0, \mathcal{S}) = \inf\{||p - p_0|| : p \in \mathcal{S}\}$. In addition, the distance between two sets $\mathcal{A}, \mathcal{B} \subset \mathbb{R}^3$ is defined as $\operatorname{dist}(\mathcal{A}, \mathcal{B}) = \inf\{||p_1 - p_2|| : p_1 \in \mathcal{A}, p_2 \in \mathcal{B}\}$. A solution $\xi(t)$ converges to a set $\mathcal{A}$ as t approaches infinity if for each $\epsilon > 0$, there exists $T > 0$ such that $\operatorname{dist}(\xi(t), \mathcal{A}) < \epsilon,\ \forall t > T$. In addition, a solution $\xi(t)$ converges to a set $\mathcal{A}$ as t approaches $t_* < \infty$ if for each $\epsilon > 0$, there exists $\delta > 0$ such that $\operatorname{dist}(\xi(t), \mathcal{A}) < \epsilon$ when $|t - t_*| < \delta$.

Weijia Yao, Yuri A. Kapitanyuk and Ming Cao are with ENTEG, University of Groningen, the Netherlands. w.yao@rug.nl, y.kapitanyuk@ieee.org, m.cao@rug.nl. The work was supported in part by the European Research Council (ERC-CoG-771687) and the Netherlands Organization for Scientific Research (NWO-vidi-14134). Weijia Yao is funded by the China Scholarship Council.

A. 3D Guiding Vector Field

A desired 3D path $\mathcal{P} \neq \emptyset$ is described by the intersection of two surfaces [11]:

$$\mathcal{P} = \{(x, y, z) : \phi_1(x, y, z) = 0, \phi_2(x, y, z) = 0\} \subset \mathbb{R}^3, \tag{1}$$

where $\phi_i \in C^2 : \mathbb{R}^3 \to \mathbb{R},\ i = 1, 2$. The 3D guiding vector field is designed as follows

$$v(\xi) = n_1(\xi) \times n_2(\xi) - k_1 e_1(\xi) n_1(\xi) - k_2 e_2(\xi) n_2(\xi) \tag{2}$$

in $\mathbb{R}^3$, where $n_i(\xi) = \nabla\phi_i(\xi)$, $e_i(\xi) = \psi_i[\phi_i(\xi)]$ and $k_i > 0$ are constants, for $i = 1, 2$. In particular, $\psi_i \in C^1 : \mathbb{R} \to \mathbb{R}$ is an arbitrarily chosen strictly increasing function, namely $\psi_i'(\cdot) > 0$ with additionally $\psi_i(0) = 0$. Therefore, $\mathcal{P} = \{\xi \in \mathbb{R}^3 : e(\xi) = 0\}$, where $e(\xi) = [e_1(\xi)\ e_2(\xi)]^T$. It is convenient to choose $\psi_i(s) = s$, which satisfies the conditions mentioned above.

Let $\tau(\xi) = n_1(\xi) \times n_2(\xi)$, $N(\xi) = \begin{bmatrix} n_1(\xi) & n_2(\xi) \end{bmatrix}_{3\times 2}$ and $K = \begin{bmatrix} k_1 & 0 \\ 0 & k_2 \end{bmatrix}$. Now (2) can be re-written compactly as

$$v(\xi) = \tau(\xi) - N(\xi) K e(\xi). \tag{3}$$

The integral curves of (3) correspond to the trajectories of the following autonomous ordinary differential equation (ODE):

$$\frac{\mathrm{d}}{\mathrm{d}t}\xi(t) = v(\xi(t)), \quad t \geq 0, \tag{4}$$

where $\xi(t) : t \mapsto (x, y, z)$. Since the differentiability class of the right part of (4) is C^1, the local existence and uniqueness of the solution of (4) is guaranteed. We want to investigate the properties of the integral curves of the vector field (3) corresponding to the solution of (4).

Remark 1: Note that the definition of $\mathcal{P}$ in (1) does not imply that the intersection of two surfaces is a single connected curve. In fact, $\mathcal{P}$ may represent several disjoint curves or even a plane. Nevertheless, the proofs in the following text are still valid as long as the assumptions are satisfied. In fact, under Assumption 1 discussed later, $\mathcal{P}$ is guaranteed to be a one-dimensional embedded submanifold in $\mathbb{R}^3$ as Lemma 1 states. However, in the context of the path following problem, we tend to choose suitable ϕ_i such that this manifold is of single branch too.

Remark 2: The reason to introduce the error function $\psi(\cdot)$ is that it may be desirable that $\psi_i'(s)|_{s=\phi_i}$ are topologically similar so that the trajectory can approach the given two surfaces at a similar rate, and thus converge to the desired path. However, for conciseness and simplicity, in this paper, we assume $\psi_i(s) = s$. In other words, the error function is described by $e_i(\xi) = \phi_i(\xi)$.

B. Assumptions

We define a set

$$\mathcal{M} = \{\xi \in \mathbb{R}^3 : N(\xi) K e(\xi) = 0\}. \tag{5}$$

This set contains the desired path $\mathcal{P}$, i.e., $\mathcal{P} \subset \mathcal{M}$. Furthermore, a **critical set** is defined as

$$\mathcal{C} = \{\xi \in \mathcal{M} : \mathrm{rank}(N(\xi)) \leq 1\}. \tag{6}$$

At these critical points (the elements of the critical set), the vector field degenerates, i.e., $v(\xi) = 0$. Also note that $\mathcal{C}$ equals the set of the equilibrium points of (4), that is, $\mathcal{C} = \{\xi \in \mathbb{R}^3 : \dot{\xi}(t) = v(\xi) = 0\}$. This can be seen from the fact that if $n_1(\xi)$ and $n_2(\xi)$ are linearly independent, then they are also linearly independent with $n_1(\xi) \times n_2(\xi)$. Since the coefficient of $n_1(\xi) \times n_2(\xi)$ is non-zero, it can be concluded that $\dot{\xi}(t) = v(\xi) \neq 0$. Therefore, the linear dependence of $n_1(\xi)$ and $n_2(\xi)$ is a also necessary condition for ξ to be an equilibrium point of (4).

Since the set $\mathcal{T} = \{\xi \in \mathcal{M} : \mathrm{rank}(N(\xi)) = 2\} \subset \mathcal{P}$, it follows that $\mathcal{P} \cup \mathcal{C} = \mathcal{M}$. However, it is desirable that $\mathcal{T} = \mathcal{P}$ so that the desired path does not contain any points from the critical set. So we make the following assumption.

Assumption 1: $\mathrm{dist}(\mathcal{C}, \mathcal{P}) > 0$.

This assumption implies that for any point $\xi \in \mathcal{P}$, $n_1(\xi)$ and $n_2(\xi)$ are linearly independent. Specifically, we have the following lemma.

Lemma 1: Under Assumption 1, $\mathcal{P}$ is a C^2 embedded submanifold in $\mathbb{R}^3$.

Proof: Denote $\Phi(\xi) = [\phi_1(\xi)\ \phi_2(\xi)]^T$. So $\Phi : \mathbb{R}^3 \to \mathbb{R}^2$, and $\mathcal{P} = \Phi^{-1}(0)$ is the preimage of Φ due to the definition in (1). Under Assumption 1, for any $\xi \in \mathcal{P}$, the Jacobian matrix $\frac{d\Phi}{d\xi} = N^T(\xi)$ is of full rank. Therefore, 0 is a regular value of Φ and $\mathcal{P}$ is a C^2 embedded submanifold in $\mathbb{R}^3$ [12, Corrollary 5.14]. ■

The second assumption guarantees that the signed error function $e(p),\ p \in \mathbb{R}^3$, can be used to measure how "close" a trajectory is to the desired path. Thus, the vanishing of the error, $\lim_{t\to\infty} ||e(p(t))|| = 0$, implies the convergence to the path $\lim_{t\to\infty} \mathrm{dist}(p(t), \mathcal{P}) = 0$.

Assumption 2: For any given constant $\kappa > 0$ and $p \in \mathbb{R}^3$, it follows that

$$\inf\{||e(p)|| : \mathrm{dist}(p, \mathcal{P}) \geq \kappa\} > 0. \tag{7}$$

Similarly, as can be seen from the definition of the set $\mathcal{M}$ in (5), we also require that the vanishing of the error, i.e., $\lim_{t\to\infty} ||N(p(t))Ke(p(t))|| = 0$, implies the convergence to the set $\mathcal{M}$. This is formulated in the following assumption.

Assumption 3: For any given constant $\kappa > 0$ and $p \in \mathbb{R}^3$, it follows that

$$\inf\{||N(p)Ke(p)|| : \mathrm{dist}(p, \mathcal{M}) \geq \kappa\} > 0. \tag{8}$$

III. Convergence of Trajectories

In this section, the convergence results of the integral curves of (4) for bounded and unbounded desired 3D path are discussed.

A. Bounded Desired Path

For the bounded desired path, it is proved that the integral curves of (4) converge to either the desired path or the critical set as the solution is prolonged to infinity. Note that in this case, only Assumption 1 and 2 are adopted.

Theorem 1 (Local convergence): Let $\xi(t)$ be the solution to (4). If $\mathcal{P}$ is bounded, $\xi(t)$ will converge to the set $\mathcal{M} = \{p \in \mathbb{R}^3 : N(p)Ke(p) = 0\}$ as $t \to \infty$. Particularly, two outcomes are possible:

1) $\lim_{t\to\infty} \text{dist}(\xi(t), \mathcal{P}) = 0$, that is, the solution converges to the desired path as $t \to \infty$,
2) $\lim_{t\to\infty} \text{dist}(\xi(t), \mathcal{C}) = 0$, that is, the solution converges to the critical set as $t \to \infty$.

Proof: The derivative of e with respect to t is:

$$\begin{aligned}\dot{e}(\xi(t)) &= N^T(\xi(t))\dot{\xi}(t) \\ &= N^T(\xi(t))v(\xi(t)) \\ &= -N^T(\xi(t))N(\xi(t))Ke(\xi(t)).\end{aligned} \tag{9}$$

Note that the above result has utilized the property that $N^T(\xi(t))\tau(\xi(t)) = 0$. Now we define a Lyapunov function candidate by

$$V(e(\xi(t))) = 1/2\ e^T(\xi(t))Pe(\xi(t)), \tag{10}$$

where P is a symmetric positive definite matrix. Then $V > 0$ on $\mathbb{R}^3\backslash\mathcal{P}$. Taking the derivative of V with respect to t we obtain:

$$\begin{aligned}\dot{V}(e(\xi(t))) &= 1/2\ (\dot{e}^T(\xi(t))Pe(\xi(t)) + e^T(\xi(t))P\dot{e}(\xi(t))) \\ &= -\frac{1}{2}e^T(\xi(t))Qe(\xi(t)),\end{aligned} \tag{11}$$

where $Q = K^TN^T(\xi(t))N(\xi(t))P + PN^T(\xi(t))N(\xi(t))K$. Let $P = K$, which is positive definite, then $\dot{V}(\xi(t)) = -||N(\xi(t))Ke(\xi(t))||^2 \leq 0$ on $\mathbb{R}^3\backslash\mathcal{P}$.

Given $r > 0$, a ball is defined by $\mathcal{B}_r = \{\xi \in \mathbb{R}^3 : ||\xi|| \leq r\} \subset \mathbb{R}^3$. Since $\mathcal{P}$ is bounded, r can be chosen sufficiently large such that $\xi(t)|_{t=0} \in \mathcal{B}_r$, $\mathcal{P} \subset \mathcal{B}_r$, and $\alpha = \min_{||\xi||=r} V(e(\xi)) > 0$. Take $\beta \in (0, \alpha)$ and let

$$\Omega_\beta = \{\xi \in \mathcal{B}_r : V(e(\xi)) \leq \beta\}. \tag{12}$$

Obviously, Ω_β is in the interior of $\mathcal{B}_r$ and it is compact. Hence, (4) has a unique solution defined for all $t \geq 0$ whenever $\xi(0) \in \Omega_\beta$. Moreover, Ω_β is positively invariant since $\dot{V}(\xi(t)) \leq 0$. Let $\mathcal{A} = \{\xi \in \Omega_\beta : \dot{V}(\xi) = 0\} = \{\xi \in \Omega_\beta : N(\xi)Ke(\xi) = 0\} \subset \mathcal{M}$. Next we are going to prove that the largest invariant set in $\mathcal{A}$ is itself. Note that $\mathcal{A}$ is the union of two sets, i.e., $\mathcal{A} = \mathcal{A}_1 \cup \mathcal{A}_2$, where $\mathcal{A}_1 = \{\xi \in \mathcal{A} : \text{rank}(N(\xi)) \leq 1\}$ and $\mathcal{A}_2 = \{\xi \in \mathcal{A} : \text{rank}(N(\xi)) = 2\}$. We consider the solutions of (4) starting from these two sets respectively.

1) When the trajectory starts from $\mathcal{A}_1$, i.e., $\xi(0) \in \mathcal{A}_1$, $n_1(\xi(0))$ and $n_2(\xi(0))$ are linearly dependent (this includes the case where either of them is zero). Thus (4) indicates that $\dot{\xi}(t)|_{t=0} = 0$. Since the solution of (4) exists and is unique, $\xi(0) \in \mathcal{A}_1 \Rightarrow \xi(t) \equiv \xi(0) \in \mathcal{A}_1,\ t \geq 0$.
2) When the trajectory starts from $\mathcal{A}_2$, i.e., $\xi(0) \in \mathcal{A}_2$, $n_1(\xi(0))$ and $n_2(\xi(0))$ are linearly independent. Then (4) becomes $\dot{\xi}(t)|_{t=0} = \tau$, which is the tangent vector of $\mathcal{P}$ at $\xi(0)$. According to Lemma 1 and the existence and uniqueness of solutions of ordinary differential equations on manifolds (e.g. [11]), the trajectory $\xi(t)$ will not leave $\mathcal{P}$, or $\mathcal{A}_2$. That is, $\xi(0) \in \mathcal{A}_2 \Rightarrow \xi(t) \in \mathcal{A}_2,\ t \geq 0$.

The above discussion concludes that $\mathcal{A}$ is itself the largest invariant set. Then according to LaSalle's invariance principle (e.g. [13, Theorem 4.4]), every solution $\xi \in \mathbb{R}^3$ starting in Ω_β approaches $\mathcal{A} \subset \mathcal{M}$ as $t \to \infty$. Since $\mathcal{A}_1 \subset \mathcal{C}$, $\mathcal{A}_2 \subset \mathcal{P}$ and $\text{dist}(\mathcal{C}, \mathcal{P}) > 0$ (by Assumption 1), it follows that $\text{dist}(\mathcal{A}_1, \mathcal{A}_2) > 0$ and particularly, the solution converges either to the desired path or the critical set as $t \to \infty$. ■

Theorem 2 (Global convergence): Let $\xi(t)$ be the solution to (4). If $\mathcal{P}$ is bounded and either $\phi_1(\xi)$ or $\phi_2(\xi)$ is radially unbounded with respect to ξ, $\xi(t)$ will globally converge to the set $\mathcal{M} = \{p \in \mathbb{R}^3 : N(p)Ke(p) = 0\}$ as $t \to \infty$. Particularly, two outcomes are possible:

1) $\lim_{t\to\infty} \text{dist}(\xi(t), \mathcal{P}) = 0$, that is, the solution globally converges to the desired path,
2) $\lim_{t\to\infty} \text{dist}(\xi(t), \mathcal{C}) = 0$, that is, the solution globally converges to the critical set.

Proof: The proof is similar to that of Theorem 1. However, since $\phi_i(\xi)$ is radially unbounded with respect to ξ, that is, $\phi_i(\xi) \to \infty$ as $||\xi|| \to \infty$, $V(e(\xi))$ is also radially unbounded with respect to ξ. Then the set Ω_β is bounded for all values of $\beta > 0$. Therefore, for any initial state $\xi(0)$, no matter how large $||\xi(0)||$ is, the solution $\xi(t)$ of (4) globally approaches $\mathcal{M}$ as $t \to \infty$. Then due to Assumption 1, the solution converges globally either to the desired path or the critical set. ■

B. Unbounded Desired Path

The analysis presented before for the bounded desired path cannot be directly applied to the unbounded desired path since for any ball $\mathcal{B}_r$ containing part of the desired path, $\alpha = \min_{||\xi||=r} V(e(\xi)) = 0$, so the set Ω_β is not available. Moreover, in this case, the maximum prolonged time of the solution to (4) cannot be readily derived. Nevertheless, under an additional condition and with different analysis, similar results can still be obtained.

1) Maximum Prolonged Time: Assume that $||\tau|| = ||n_1 \times n_2||$ is upper bounded by κ_b, it can be proved that the solution can be prolonged to infinity as Lemma 2 shows. This assumption is satisfied by carefully choosing ϕ_i with bounded $\|\nabla\phi_i\|$. For instance, $\phi_1 = y - \sin(x)$ and $\phi_2 = z$.

Lemma 2: If $||\tau||$ is upper bounded by $\kappa_b > 0$, the maximum interval of existence of the solution to (4) is $[0, \infty)$.

Proof: Due to page limits, the proof will be given in the full version of this paper. ■

Corollary 1: Assume that $||\tau||$ is upper bounded, then

$$\int_0^\infty ||N(\xi(t))Ke(\xi(t))||^2 dt = -\int_0^\infty \dot{V}(\xi(t))dt < +\infty. \tag{13}$$

Proof: Due to page limits, the proof will be given in the full version of this paper. ■

2) Convergence Results: As for unbounded desired path, we need Assumptions 1, 2 and 3 to draw a similar conclusion.

First we need the absolute continuity of the Lebesgue integral (Lemma 3) to reach Corollary 2 for further discussion.

Lemma 3 (absolute continuity of Lebesgue integrals [14]): If f is Lebesgue integrable on $\mathbb{R}^n$, then for any $\epsilon > 0$, there exists $\delta > 0$ such that for all measurable sets $\mathcal{D} \subset \mathbb{R}^n$ with measure $m(\mathcal{D}) < \delta$,

$$\int_{\mathcal{D}} |f| dm < \epsilon. \tag{14}$$

Now we are ready to prove the following results.

Corollary 2: For any $\epsilon > 0$, there exists $0 < \delta \leq \epsilon$ such that for all intervals with length $|\Delta| < \delta$,

$$\int_{\Delta} ||N(\xi(t))Ke(\xi(t))|| dt < 2\epsilon.$$

Proof: Due to page limits, the proof will be given in the full version of this paper. ■

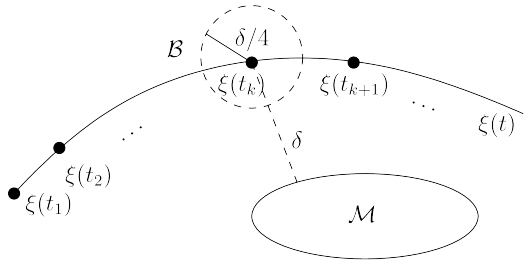

Fig. 1. The illustration of the proof of Theorem 3.

Theorem 3 (Global convergence): Let $\xi(t)$ be the solution to (4). If $\mathcal{P}$ is unbounded and $||\tau||$ is upper bounded by $\kappa_b > 0$, $\xi(t)$ will converge to the set $\mathcal{M} = \{p \in \mathbb{R}^3 : N(p)Ke(p) = 0\}$ as $t \to \infty$. Particularly, two outcomes are possible:

1) $\lim_{t\to\infty} \text{dist}(\xi(t), \mathcal{P}) = 0$, that is, the solution converges to the desired path as $t \to \infty$,
2) $\lim_{t\to\infty} \text{dist}(\xi(t), \mathcal{C}) = 0$, that is, the solution converges to the critical set as $t \to \infty$.

Proof: Define the Lyapunov function candidate $V(\xi(t))$ as in Theorem 1 and denote $\eta(\xi(t)) = ||N(\xi(t))Ke(\xi(t))||$. Suppose $\xi(t)$ does not converge to $\mathcal{M}$, then there exists a sequence $\{t_k\}$, and $t_k \to \infty$ as $k \to \infty$, such that (due to Assumption 3)

$$\text{dist}(\xi(t_k), \mathcal{M}) > \delta > 0 \Rightarrow \eta(\xi(t_k)) > \epsilon > 0. \tag{15}$$

Therefore, $\dot{V}(\xi(t_k)) = -\eta^2(\xi(t_k)) < -\epsilon^2$. According to Assumption 3, there exists $\epsilon' > 0$ such that when $\text{dist}(\xi, \mathcal{M}) > \delta/2$, one has $\eta(\xi) > \epsilon'$. Since $\text{dist}(\xi(t_k), \mathcal{M}) > \delta$, given a ball $\mathcal{B}(\xi(t_k), \delta/4)$, then for any $y \in \mathcal{B}(\xi(t_k), \delta/4)$, it follows that (see Fig. 1)

$$\text{dist}(y, \mathcal{M}) > \delta/2 \Rightarrow \dot{V}(y) < -\epsilon'^2. \tag{16}$$

Taking $\epsilon = \frac{\delta}{2(2+\kappa_b)}$ in Corollary 2, then there exists an interval Δ with length $|\Delta| < \epsilon$ such that

$$\begin{aligned}\int_{\Delta} ||\dot{\xi}(t)|| dt &= \int_{\Delta} ||\tau(\xi(t)) - N(\xi(t))Ke(\xi(t))|| dt \\ &\leq \int_{\Delta} ||\tau(\xi(t))|| dt + \int_{\Delta} ||N(\xi(t))Ke(\xi(t))|| dt \\ &\leq (\kappa_b + 2)\epsilon < \frac{\delta}{2}.\end{aligned}$$

Then it follows that $\xi[t_k - \Delta/2, t_k + \Delta/2] \subset \mathcal{B}(\xi(t_k), \delta/4)$. Therefore,

$$\int_{t_k-\Delta/2}^{t_k+\Delta/2} \dot{V}(\xi(t)) dt < -\epsilon'^2 \Delta. \tag{17}$$

This leads to

$$\begin{aligned}\int_0^{\infty} \dot{V}(\xi(t)) dt &\leq \sum_{k=1}^{\infty} \int_{t_k-\Delta/2}^{t_k+\Delta/2} \dot{V}(\xi(t)) dt \\ &\leq -\sum_{k=1}^{\infty} \epsilon'^2 \Delta \leq -\infty,\end{aligned} \tag{18}$$

which contradicts Corollary 1. Therefore, $\xi(t)$ converges to $\mathcal{M}$ as $t \to \infty$. Then due to Assumption 1, the solution converges either to the desired path or the critical set. ■

Remark 3: For the case of unbounded desired path, the results presented above is valid under the condition that $||\tau||$ is upper bounded by κ_b. This seems restrictive. However, by introducing a *smooth bounding operator* $f_b : \mathbb{R}^n \to \mathbb{R}^n$, $||f_b(\tau)||$ can be guaranteed to be bounded and additionally, $f_b(\tau)$ is smooth. For example, $f_b(\xi) = \frac{\xi}{1+||\xi||^2}$, where $\xi \in \mathbb{R}^3$ and the upper bound is $1/2$. However, $||f_b(\xi)||$ vanishes as $||\xi|| \to \infty$. Another better choice of the smooth bounding operator contains a bump function. Note that the smooth bounding operator neither changes the direction of $n_1 \times n_2$ nor affects the speed of the convergence to the desired path, which is dominated by the unmodified latter term as can be seen from the time derivative of the Lyapunov function in Theorem 1. Nevertheless, for practical reasons, it is desirable to normalize the original guiding vector field, albeit possibly leading to finite escape time. Due to page limits, the analysis will be given in the full version of this paper.

IV. Illustrative Examples

In the previous sections, we have proved that based on Assumptions 1, 2 and 3, the trajectory either converges to the desired path or the critical set. However, it is desirable that the set of trajectories which converge to the critical set is of measure zero. Then in this case, convergence to the desired path is almost globally guaranteed. For the 3D path following problem, it is still difficult to draw this conclusion without given explicit forms of ϕ_1 and ϕ_2. Even for the same desired path, different choices of ϕ_1 and ϕ_2 will lead to contrary results. In this section, examples are provided to illustrate the idea and verify the previous theorems. First, a definition and a lemma are provided for further discussion.

Definition 1 ([10], stable manifold): Let $\xi^* \in \mathcal{C}$ be a critical point, and thus an equilibrium point of (4). The stable manifold of ξ^*, denoted by $\mathcal{W}(\xi^*)$, is the set of all points

ξ_0 such that the solution of (4), starting at $\xi(0) = \xi_0$, exists for all $t \geq 0$ and $\lim_{t\to\infty} \xi(t) = \xi^*$.

The following lemma is a corollary of the center manifold theorem [15]. It provides an approach to determine whether the stable manifold of a critical point is of measure zero.

Lemma 4: If there is at least one strictly unstable eigenvalues of the Jacobian matrix $J(\xi^*) = \left.\frac{\partial v(\xi)}{\partial \xi}\right|_{\xi=\xi^*}$, i.e., $\exists\, i$, such that $\mathrm{Re}(\lambda_i(J(\xi^*))) > 0$, then $\mathcal{W}(\xi^*)$ is of measure zero. Furthermore, if all of the eigenvalues are strictly unstable, then $\mathcal{W}(\xi^*) = \{\xi^*\}$.

Examples of a bounded desired path and an unbounded desired path are provided. In addition, a counter-example representing the same unbounded desired path is also discussed, albeit with divergent trajectories. We use the normalized guiding vector field for the simulations.

A. Bounded Desired Path

Consider

$$\phi_1(x, y, z) = (x - a)^2 + (y - b)^2 - r^2,$$
$$\phi_2(x, y, z) = y^2 + z^2 - R^2,$$

where $a, b, R, r \in \mathbb{R}$ and $R > r > 0$. $\phi_i = 0, i = 1, 2$, is the surface of a cylinder, which we refer to as the first and second surface here. The shape of the desired path varies subject to different values of b. In this example, it is assumed that $b \in (-R-r, -R+r) \cup (R-r, R+r)$, and thus, for example, the intersection 3D curve is a closed black line in Fig. 2(a). In this case, the critical set $\mathcal{C}$ consists of a finite number of isolated points. By definition, $n_1 = 2\begin{bmatrix} x-a & y-b & 0 \end{bmatrix}^T$ and $n_2 = 2\begin{bmatrix} 0 & y & z \end{bmatrix}^T$. According to the definition of $\mathcal{C}$, one considers the set of points which satisfies $\mathrm{rank}(N(\xi)) \leq 1$. In fact, they are three straight lines, denoted by L_1, L_2 and L_3, whose points satisfy respectively (a, b, z), $(x, 0, 0)$ and $(a, y, 0)$, where x, y, z are to be determined. L_1 and L_2 turn out to be the symmetric lines of the surfaces of the cylinder. In addition, at each point of L_3, the nonzero gradient vectors are parallel, i.e., $n_1(\xi) \parallel n_2(\xi)$.

Suppose now $a = 0$, $b = 1.5$, $R = 2$, $r = 1$ and $k_1 = k_2 = 1$. It can be calculated that there are three isolated critical points in total, with two points on L_1 and one point on L_3 (see red plus signs in Fig. 2(a) and Fig. 2(b)). For each of the critical points, the eigenvalues of the corresponding Jacobian matrix have at least one strictly unstable eigenvalue. Then it can be concluded that the stable manifold of each of the critical points is of measure zero. So the trajectory will almost globally converge to the desired path. In particular, in Fig. 2(a), the trajectory starts from $(a, -2, 0)$ on L_3, then it will converge to the critical point on that line. In fact, for each point ξ except for the critical point on L_3, the vector field $v(\xi)$ is parallel to this line, and thus once the trajectory starts from a point on this line, it will not leave it. One may assume that this is also true when the trajectory starts from a point on L_1 or L_2. However, this is in fact not true for L_1 or L_2 (see Fig. 2(b)). In this case, taking L_1 for example, for each point ξ except for the critical point on L_1, the vector field is not parallel to L_1. Instead, it "pulls" the trajectory to get closer to the second surface. In Fig. 2(b), the trajectory starts from $(a, b, 2.5)$ but converges to the desired path. Fig. 2(c) illustrates the error.

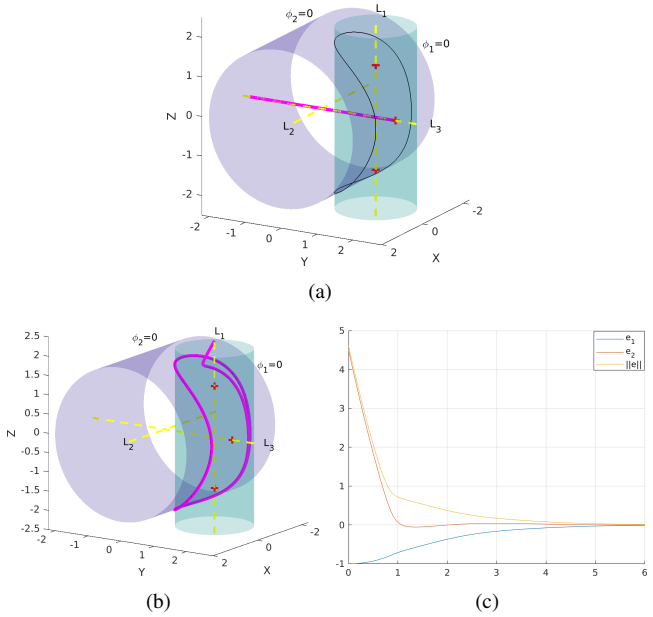

(a) (b) (c)

Fig. 2. Example 1: a bounded desired path. Trajectories (pink) converge to a critical point (a) and to the desired path (b) respectively.

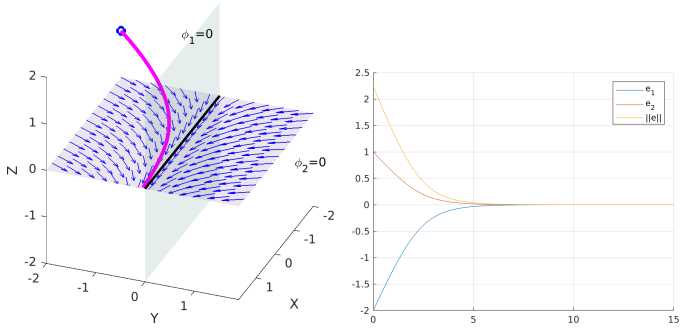

(a) (b)

Fig. 3. Example 2: an unbounded desired path. The trajectories (pink) converges to the desired straight line. The blue circle is the starting point.

B. Unbounded Desired Path

Consider a simple unbounded desired path - a straight line described by the intersection of two zero-level surfaces.

$$\phi_1(x, y, z) = y, \quad \phi_2(x, y, z) = z.$$

It is easy to find out that in this case, the critical set is empty. So the trajectory will always converge to the desired path as $t \to \infty$. Fig. 3(a) shows that the trajectory starting from $(-2, -2, 1)$ converges to the desired line, and the errors are plotted in Fig. 3(b). Note that for clarity, only the vector field in the $z = 0$ plane is plotted. However, given the same desired path, but with different $\phi_i, i = 1, 2$, the result can be distinctly different. Consider

$$\phi_1(x, y, z) = ye^{-x}, \quad \phi_2(x, y, z) = z.$$

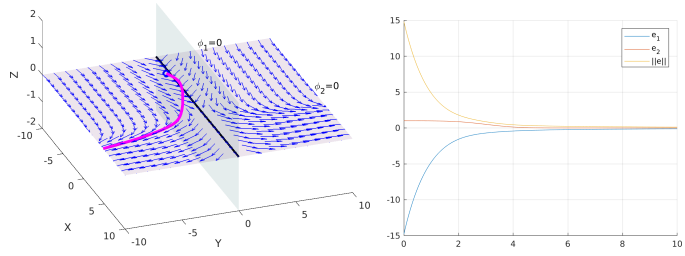

(a) (b)

Fig. 4. Example 3: the same unbounded desired path as Example 2. However, the trajectories (pink) does not converge to the desired straight line. The blue circle is the starting point.

The desired path described by $(\phi_1(\xi) = 0) \cap (\phi_2(\xi) = 0)$ is the same straight line as the previous one. Nevertheless, when the trajectory starts from $(-2, -2, 1)$, it will not converge the desired path though the norm of the error $||e||$ is vanishing (see Fig. 4(a) and Fig. 4(b)). Note that this does not conflict with the theorems in this paper, because this case does not satisfy Assumption 2 and 3. From this example it can be manifested that given the same desired path, with different ϕ_i, the convergence results can be even opposite. The assumptions somehow provides criteria to choose "suitable" ϕ_i. Another interesting example is an unbounded spiral, where we can choose $\phi_1 = x - \cos(z)$ and $\phi_2 = y - \sin(z)$. Since there are no critical points, the trajectory will globally converge to the desired path.

V. Conclusion and Future Work

This paper has provided a unified approach to the local and global analysis of the 3D vector field for both bounded and unbounded desired paths. The questions of the existence of solutions and the convergence of the integral lines generated by the 3D vector field are rigorously and comprehensively studied. It has been proved that, under the assumptions proposed in this paper, the trajectory will converge either to the desired path or to the critical set, while for the normalized 3D vector field, it will possibly converge to the critical set in finite time. Note that if the stable manifold of a critical point is of measure zero, then the path-convergence is almost globally guaranteed. Interestingly, a critical point happens to be an equilibrium point of (4), so the path following problem is converted to proving that these equilibrium points are unstable.

Note that the investigation of the solution to the ODE (4) is significant for robotics application. This is justified as follows. Typically, a path-following controller contains two sub-controllers, the outer one (kinematics) which takes the states of the robot as input and calculates the desired generalized velocities as output to the inner controller, and the inner one (dynamics) which takes the desired generalized velocities as input and computes the corresponding force or toque as output to the robot. Assume that the inner (dynamics) controller is sufficiently fast and precise, we may consider the generalized velocities as the control inputs to the robot. Therefore, the robot model can be described by a simple kinematics model, such as a single-integrator model: $\frac{\mathrm{d}}{\mathrm{d}t}\xi(t) = u(t)$, where $\xi(t) \in \mathbb{R}^3$ is the coordinate of the robot and $u(t)$ is the control input at time t. Let $u(t) = v(\xi(t))$, where v is the vector field function as discussed before, and then we only need to study the solution to (4). Even for a nonholonomic robot model, this result is still useful [5].

Although Lemma 4 can be used to check the stability of the critical points, a general analytic approach related to the forms of ϕ_i remains challenging. A more realistic model of the robot, such as a nonholonomic model with constant moving speeds, and the effects of different error functions $\psi(\cdot)$ will also be considered in the future work.

Acknoledgements

Weijia Yao would like to thank Bohuan Lin for the valuable technical discussions.

References

[1] B. Siciliano and O. Khatib, *Springer Handbook of Robotics*. Secaucus, NJ, USA: Springer-Verlag New York, Inc., 2007.

[2] P. B. Sujit, S. Saripalli, and J. B. Sousa, "Unmanned aerial vehicle path following: A survey and analysis of algorithms for fixed-wing unmanned aerial vehicless," *IEEE Control Systems*, vol. 34, no. 1, pp. 42–59, Feb 2014.

[3] Y. Liang and Y. Jia, "Combined vector field approach for 2d and 3d arbitrary twice differentiable curved path following with constrained uavs," *Journal of Intelligent & Robotic Systems*, vol. 83, no. 1, pp. 133–160, 2016.

[4] K. Łakomy and M. M. Michałek, "The vfo path-following kinematic controller for robotic vehicles moving in a 3d space," in *Robot Motion and Control (RoMoCo), 2017 11th International Workshop on*. IEEE, 2017, pp. 263–268.

[5] V. M. Goncalves, L. C. A. Pimenta, C. A. Maia, B. C. O. Dutra, and G. A. S. Pereira, "Vector fields for robot navigation along time-varying curves in n -dimensions," *IEEE Transactions on Robotics*, vol. 26, no. 4, pp. 647–659, Aug 2010.

[6] D. R. Nelson, D. B. Barber, T. W. McLain, and R. W. Beard, "Vector field path following for miniature air vehicles," *IEEE Transactions on Robotics*, vol. 23, no. 3, pp. 519–529, June 2007.

[7] S. Griffiths, "Vector field approach for curved path following for miniature aerial vehicles," in *AIAA guidance, navigation, and control conference and exhibit*, 2006, p. 6467.

[8] S. Zhu, D. Wang, and C. B. Low, "Ground target tracking using uav with input constraints," *Journal of Intelligent & Robotic Systems*, vol. 69, no. 1, pp. 417–429, Jan 2013.

[9] Y. A. Kapitanyuk, S. A. Chepinskiy, and A. A. Kapitonov, "Geometric path following control of a rigid body based on the stabilization of sets," *IFAC Proceedings Volumes*, vol. 47, no. 3, pp. 7342 – 7347, 2014, 19th IFAC World Congress.

[10] Y. A. Kapitanyuk, A. V. Proskurnikov, and M. Cao, "A guiding vector-field algorithm for path-following control of nonholonomic mobile robots," *IEEE Transactions on Control Systems Technology*, vol. 26, no. 4, pp. 1372–1385, July 2018.

[11] M. P. Do Carmo, *Differential Geometry of Curves and Surfaces: Revised and Updated Second Edition*. Courier Dover Publications, 2016.

[12] J. Lee, *Introduction to Smooth Manifolds: Second Edition*, ser. Graduate texts in mathematics. Springer, 2015.

[13] H. K. Khalil, "Noninear systems," *Prentice-Hall, New Jersey*, vol. 2, no. 5, pp. 5–1, 1996.

[14] F. Jones, *Lebesgue integration on Euclidean space*. Jones & Bartlett Learning, 2001.

[15] R. Potrie and P. Monzon, "Local implications of almost global stability," *Dynamical Systems*, vol. 24, no. 1, pp. 109–115, 2009.